Exp Brain Res (2015) 233:2869–2882
DOI 10.1007/s00221-015-4357-y

RESEARCH ARTICLE

Wideband phase locking to modulated whisker vibration point to a temporal code for texture in the rat's barrel cortex

Tobias A. S. Ewert[1,2] · Johannes Möller[1] · Andreas K. Engel[1] · Christiane Vahle-Hinz[1]

Received: 28 August 2014 / Accepted: 9 June 2015 / Published online: 1 July 2015

Abstract Rats probe objects with their whiskers and make decisions about sizes, shapes, textures and distances within a few tens of milliseconds. This perceptual analysis requires the processing of tactile high-frequency object components reflecting surface roughness. We have shown that neurons in the barrel cortex of rats encode high-frequency sinusoidal vibrations of whiskers for sustained periods when presented with constant amplitudes and frequencies. In a natural situation, however, stimulus parameters change rapidly when whiskers are brushing across objects. In this study, we therefore analysed cortical responses to vibratory movements of single whiskers with rapidly changing amplitudes and frequencies. The results show that different neural codes are employed for a processing of stimulus parameters. The frequency of whisker vibration is encoded by the temporal pattern of spike discharges, i.e., the phase-locked responses of barrel cortex neurons. In addition, oscillatory gamma band activity was induced during high-frequency stimulation. The pivotal descriptor of the amplitude of whisker displacement, the velocity, is reflected in the rate of spike discharges. While phase-locked discharges occurred over the entire range of frequencies tested (10–600 Hz), the discharge rate increased with stimulus velocity only up to about 60 µm/ms, saturating at a mean rate of ~117 spikes/s. In addition, the results show that whisker movements of more than 500 Hz bandwidth may be encoded by phase-locked responses of small groups of cortical neurons. Thus, even single whiskers may transmit information about wide ranges of textural components owing to their set of different types of hair follicle mechanoreceptors.

Keywords Anaesthesia · Electrophysiology · High-frequency vibration · Tactile processing · Oscillation

✉ Christiane Vahle-Hinz
vahle-hinz@uke.uni-hamburg.de

[1] Department of Neurophysiology and Pathophysiology, University Medical Center Hamburg-Eppendorf, Martinistr. 52, 20246 Hamburg, Germany

[2] Department of Neurology, University Medical Center Hamburg-Eppendorf, Martinistr. 52, 20246 Hamburg, Germany

Introduction

Several mechanisms have been discussed recently to explain the astounding ability of rats to rapidly and reliably discriminate among fine-grained textures (Guic-Robles et al. 1989; Carvell and Simons 1990; Krupa et al. 2001). One view is that the various features of an object's surface are encoded by a set of whiskers each of which having its own distinct mechanical properties, and that cortical mechanisms are required to integrate these multiple spatially and temporally distributed sensory representations (Hartmann et al. 2003; Neimark et al. 2003; Andermann et al. 2004; Metha and Kleinfeld 2004; Moore 2004). Another view suggests that individual whiskers may translate textures across a broad range of spatiotemporal frequencies into different vibration profiles (Hipp et al. 2006; Lottem and Azouz 2008, 2009) which are represented in the rate (Arabzadeh et al. 2003, 2006) or temporal pattern of spike discharges (Gibson and Welker 1983; Deschênes et al. 2003; Jones et al. 2004a, b, 2006; Arabzadeh et al. 2006).

Whiskers have indeed been shown to translate surface roughness into distinct high-frequency micro motions, which elicit closely correlated spiking activity in trigeminal ganglion neurons (Gibson and Welker 1983; Jones et al. 2004a, b, 2006; Lottem and Azouz 2008, 2009; Bale et al. 2013). This suggests that the micro motions induce

phase-locked receptor potentials in the mechanoreceptors of the sinus hair follicles. This most likely is enabled by the alignment of the mechanoreceptors along the hair shaft with tight coupling via an especially tough basement membrane at the epidermal–dermal border, the glassy membrane (Andres 1966; Rice et al. 1997). As a result, the generation of action potentials was shown to follow stimulus transients in a phase-locked manner up to 1 kHz (Deschênes et al. 2003) or 2.8 kHz in cats (Gottschaldt and Vahle-Hinz 1981). The delay caused by the mechanoelectric transduction process was measured to be ~0.2 ms, and the phase jitter of action potentials occurring in response to a 1 kHz vibration was <10 µs (Gottschaldt and Vahle-Hinz 1981).

It may be assumed that such an extraordinary sensitivity of peripheral sensors for high-frequency motions is deployed for perception, rather than being dismissed by the system. For the whisker-to-barrel pathway, this appears likely as information on timing and high-frequency components of whisker movements are preserved with high precision in the ascending pathway at the second (principal trigeminal nucleus) and third neuronal stages (thalamic ventral posteromedial nucleus, VPM) (Vahle-Hinz and Gottschaldt 1983; Deschênes et al. 2003; Jones et al. 2004b, 2006; Montemurro et al. 2007; Vahle-Hinz et al. 2007). What is currently missing is a demonstration that cortical neurons are capable of encoding varied high-frequency components of textures. In fact, most reports deny barrel cortex neurons such a capability (Garabedian et al. 2003; Khatri et al. 2004; Kleinfeld et al. 2006). We have reported previously that sinusoidal vibration of whiskers up to 700 Hz induced phase-locked cortical responses (Ewert et al. 2008). Our present data provide evidence that rapidly changing high-frequency stimulus features may be encoded as well thereby opening new vistas on texture discrimination in the barrel cortex.

Materials and methods

Surgical preparation

This study was performed in accordance with the EU Directive 2010/63/EU on the protection of animals used for scientific purposes and after approval by the Hamburg Administration of Health and Consumer Protection on 11 adult male *Wistar rats* (~400 g body weight) using the same methods as reported previously (Ewert et al. 2008; Vahle-Hinz et al. 2007). Anaesthesia was induced by inhalation of isoflurane via a mask and continued by mechanical ventilation of the lungs via a tracheal cannula with 1.5–2.0 vol% end-tidal isoflurane in 100 % oxygen. End-tidal isoflurane as well as CO_2 concentrations were monitored continuously (Capnomac; Datex, Helsinki, Finland). Vecuronium bromide (4 mg kg^{-1} h^{-1}) was administered for muscle relaxation via a venous catheter. The heart rate was monitored continuously and the body temperature was maintained at 37.0 ± 0.5 °C by means of a heating pad. An electrocorticogram (ECoG) was displayed throughout the experiment to aid assessment of anaesthetic depth in addition to tests of absence of cardiovascular responses when noxious pinching of a paw was applied. The animal's head was mounted in a stereotaxic holder with blunt ear bars. A unilateral craniotomy was performed above the barrel cortex, the dura was removed and the exposed cortical surface was covered with agar. At the end of the experiments, the animals were killed under 4.0 vol% isoflurane with iv potassium chloride.

Neuronal recording and stimulation

Concentrations of isoflurane (0.9–1.5 vol%) were adjusted during the recording session to the individual rat's susceptibility to the anaesthetic as determined by the absence of pinch-induced movement, ECoG and cardiovascular responses. Glass-covered tungsten microelectrodes (1 MΩ impedance at 1 kHz) were inserted perpendicular to the surface of the barrel cortex, and extracellular recordings of single- and multi-units were made at depths of 50–550 µm, corresponding to cortical layers 2/3 and 4. The neuronal activity was amplified, filtered, displayed on a personal computer and stored with 25–35 kHz sampling rate on a hard disk using the Alpha-Map Data Acquisition System (Alpha Omega Engineering, Nazareth, Israel). Neurons responding with sustained spike discharges to vibratory stimuli were selected for analysis ($n = 61$).

Single whiskers were attached to the probe of a feedback-controlled electromechanical stimulator (Somedic, Stockholm, Sweden) ~5 mm from the skin. The probe was a 100-mm-long glass tube (diameter 1 mm) with a thread protruding from its end and looping around the whisker holding it in its resting position. Care was taken to insert the probe between neighbouring whiskers such that only one was stimulated. Five different kinds of sinusoidal-shaped whisker movements in rostro-caudal direction, each with a duration of 3.2 s, were applied in this experiment (Fig. 1). Three stimuli were amplitude-modulated (AM) at 60, 110 and 180 Hz stimulation frequency, starting at 300 µm amplitude, falling to 150 and then 0 µm and rising again to 150 and 300 µm, with plateau periods of 390 ms (Fig. 1A–C). Two frequency-modulated (FM) stimuli were used; these were linearly modulated from 600 to 10 Hz (descending) and 10 to 600 Hz (ascending), respectively (Fig. 1D, E). Because of technical limitations of the electromechanical stimulator, the amplitudes had to be decreased for higher frequencies and fell from 336 to 16 µm. Both the input signal actuating the stimulator (Fig. 1Da, Ea) and the output signal reflecting the actual movement of the probe were recorded (Fig. 1Db, Eb). These were identical for the

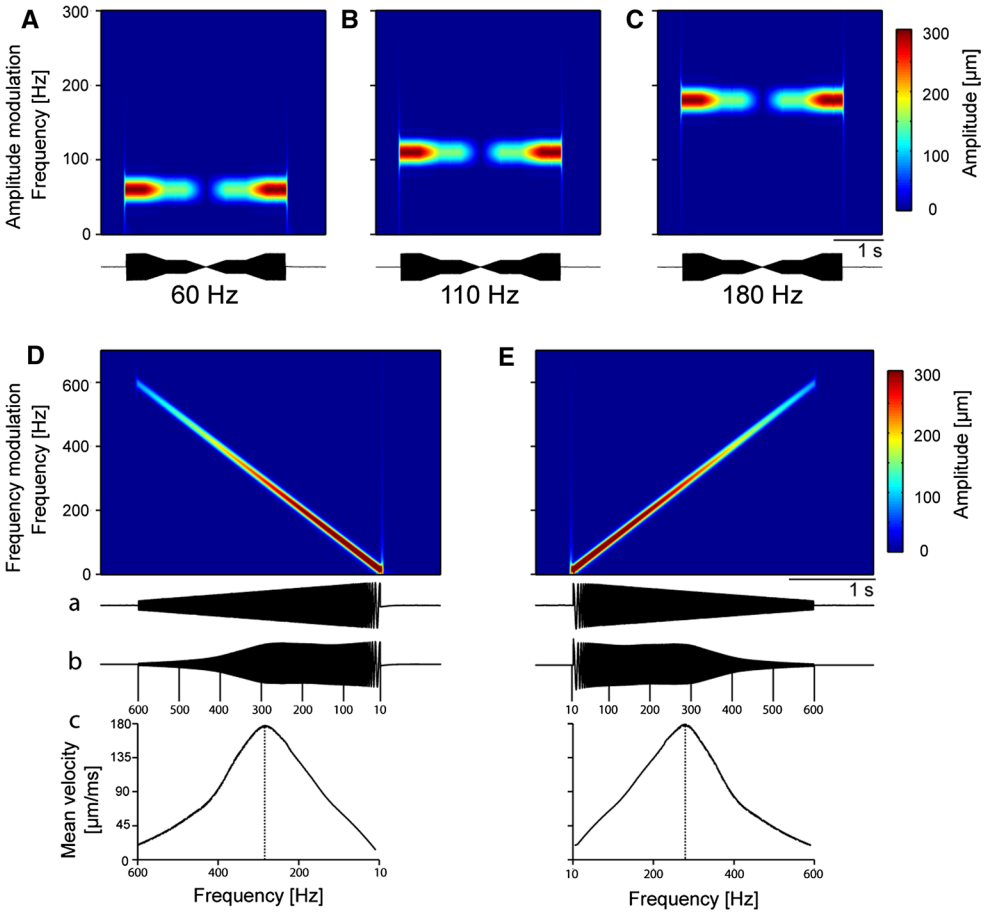

Fig. 1 The five amplitude (AM; **A**–**C**)- and frequency (FM; **D**, **E**)-modulated stimuli used in this study are shown. Frequencies and amplitudes (*colour scale*) are indicated in the time–frequency transformations and stimulus traces are displayed for each stimulus. For the FM stimuli, both the input signal to the stimulator (**Da**, **Ea**) and the actual whisker movement (**Db**, **Eb**) are shown. The profiles of the mean velocity calculated from total amplitude and duration of a half cycle of the sinusoidal movement of the FM stimuli are shown in **Dc** and **Ec**. Note that the mean velocity increases from 20 to 178 µm/ms with frequency up to 302 Hz and then decreases for higher frequencies due to the decreasing amplitude. The duration of each stimulus was 3.2 s

AM stimuli (Fig. 1A–C, lower traces), but different for the FM stimuli in terms of stimulus amplitude, therefore, only the actual whisker movement was used for calculations of amplitude and velocity (Fig. 1Dc, Ec). For each unit, the principal whisker was chosen and the five different kinds of stimuli were presented pseudo-randomly 30–50 times with interstimulus intervals of 6 s.

Data analysis

Off-line analyses were performed with programs for single-unit sorting (Offline-Sorter, Plexon, Dallas, TX, USA) for generation of time stamps and peristimulus time histograms (PSTHs; Spike2 software, Cambridge Electronic Design, UK), as well as for time–frequency analyses and statistics (custom-written Matlab routines). PSTHs (bin width 1 ms, 30–50 responses) were generated from the neuronal discharges during stimulation and during a 200-ms prestimulus period, and the response activity was calculated from the discharge rates measured at each cycle of the sinusoidal stimulus and expressed as mean discharge frequency (spikes/s) above prestimulus (ongoing) activity. A frequency-domain analysis of the spike responses was obtained by applying fast Fourier transformation (FFT; 160 ms window and 157 ms overlap) to the time stamps of the spikes transformed into continuous data with 3 kHz sampling rate. Time–frequency plots showing absolute power of the frequency components were obtained by applying FFT analysis to the mean of 30–50 consecutive responses, resulting in a measure of the evoked activity, which by definition is strictly locked to stimulus onset. Single trial FFT analysis was performed to test whether the actual stimulus frequency was reflected in single responses or resulted from summation. The induced oscillatory activity was calculated from the average of single trial FFT results after subtraction of the mean evoked response (Tallon-Baudry and Bertrand 1999). Comparisons of different responses and stimulation groups were made with ANOVA, and a $p < 0.01$ was considered significant. Data are given as mean ± SEM.

Temporal coding of stimulus frequency in cortical responses was calculated from time–frequency transformations of the evoked activity. To this end, for each point in time it was tested whether the power of the response frequency at the given vibratory frequency of whisker movement was significantly higher (ANOVA, $p < 0.05$) than the power of the same response frequency at time points when other vibratory frequencies were presented. Therefore,

for each unit the bandwidth of vibratory frequencies was determined where the temporal pattern of discharge activity reflected stimulus frequency.

Results

We analysed multi- ($n = 61$) and single-unit ($n = 19$) activity recorded in the rat's primary somatosensory cortex (S1) which was elicited by vibratory stimulation of single whiskers at modulated amplitudes (AM) and/or frequencies (FM). For AM stimuli, the amplitudes of 60, 110 and 180 Hz vibration were varied over 3.2 s in steps falling from 300 to 150 to 0 µm and rising again, with plateau periods of 390 ms ("Materials and methods" section; Fig. 1A–C). For FM stimuli, the frequencies were linearly modulated from 600 to 10 Hz (descending; "Materials and methods" section; Fig. 1D) and 10 to 600 Hz (ascending; "Materials and methods" section; Fig. 1E). All those multi-units ($n = 34$) were included in the analyses which showed, at least for one kind of stimulus, encoding of the frequency of whisker movement by the temporal pattern of neuronal discharges. Such encoding of stimulus frequency requires that phase-locked 1:1 discharges must occur over several consecutive cycles at least intermittently over the stimulus epoch [see insets of Figs. 2, 3, 6b, and single unit example in Fig. 3 of Ewert et al. (2008)]. Then, the power which reflects stimulus frequency will be significantly higher than that of other frequencies in a FFT of the response discharges (see "Materials and methods" section). By these means, encoding of information was found in responses elicited by AM whisker vibrations at 60, 110, and 180 Hz of 26, 29 and 21 multi-units, respectively. All three movement frequencies were encoded by the temporal pattern of the discharges of 20 multi-units (59 %). Moreover, adopting the same criteria, temporal coding of FM whisker vibrations was detected in 29 (85 %) multi-units for bandwidths up to 550 Hz.

Amplitude modulation

An example of a multi-unit with temporal coding of all presented AM stimuli is given in Fig. 2A–C. A typical response (original traces, Fig. 2Aa–Ca and PSTHs, Fig. 2Ab–Cb) consisted of a marked ON-burst at stimulus onset, followed by a discharge pause of about 40 ms and a subsequent rebound burst. Only then, regular discharges followed that were entrained to the whisker vibration frequency as visualized in the time–frequency plots (Fig. 2Ac–Cc) by the power increase at the stimulation frequency. The phase-locked occurrence of the multi-unit discharges is shown by the inset of Fig. 2Cb. It is noteworthy that the discharge rate decreased during stimulation with small amplitudes. The data shown for this multi-unit indicate a clear correlation of the discharge rate with the falling and rising stimulation amplitudes. The relation between discharge rate and stimulus amplitude was analysed for all multi-units by calculating the mean discharge rate for each cycle of the sinusoidal whisker movement at the three AM frequencies (Fig. 2Ad–Cd).

Falling amplitudes

There was an almost perfect linear match between discharge rate and stimulus amplitude for the stimulus part with falling amplitudes at 60 and 110 Hz vibration even during the plateau periods (Fig. 2Ad–Cd, see superimposed amplitude curve). This impression is quantified in the plots of the discharge rates as a function of stimulus amplitude (Fig. 2Ae–Ce). The positive correlation between these parameters is revealed for the falling amplitudes (filled circles) from 300 to 0 µm for 60 and 110 Hz vibration, however, for 180 Hz vibration only in the range of 158–0 µm, above which the discharge rate reached a plateau at 117.2 ± 1.9 spikes/s above prestimulus activity. The response to the first cycle at stimulus onset increased with stimulus frequency from 428.8 ± 21.4 to 518.1 ± 21.6 spikes/s ($p = 0.045$) and to 748.6 ± 54.7 spikes/s ($p < 0.0001$) for 60, 110 and 180 Hz, respectively (ANOVA Holm–Sidak method).

Rising amplitudes

For the stimulus part with rising amplitudes, the correlation between discharge rate and amplitude was not as clear. An initial increase in discharge rate was found, which became more pronounced with increasing vibration frequency (38.4 ± 3.8, 87.4 ± 9.3 spikes/s ($p < 0.0001$) and 180.9 ± 25.6 spikes/s ($p < 0.0001$), for 60, 110 and 180 Hz, respectively; ANOVA Holm–Sidak method). This is very likely a result of an ON-response marking stimulus increase largely irrespective of stimulus amplitude, rather reflecting stimulus dynamics, as is also seen in the ON-responses at stimulus onset.

Plateau responses

The plateau responses at 150 and 300 µm amplitude also increased with vibration frequency from 60 to 110 and to 180 Hz ($p = 0.05$, $p = 0.02$ for 150 µm; $p = 0.05$, $p = 0.02$ for 300 µm; ANOVA Holm–Sidak method) and were larger during falling stimuli than during rising stimuli for 110 ($p < 0.0001$) and 180 Hz ($p < 0.0001$) at 300 µm amplitude and for 180 Hz ($p < 0.0001$) at 150 µm amplitude. In addition, at 180 Hz, the plateau response at 150 µm during falling stimuli was as large as that at 300 µm during rising stimuli

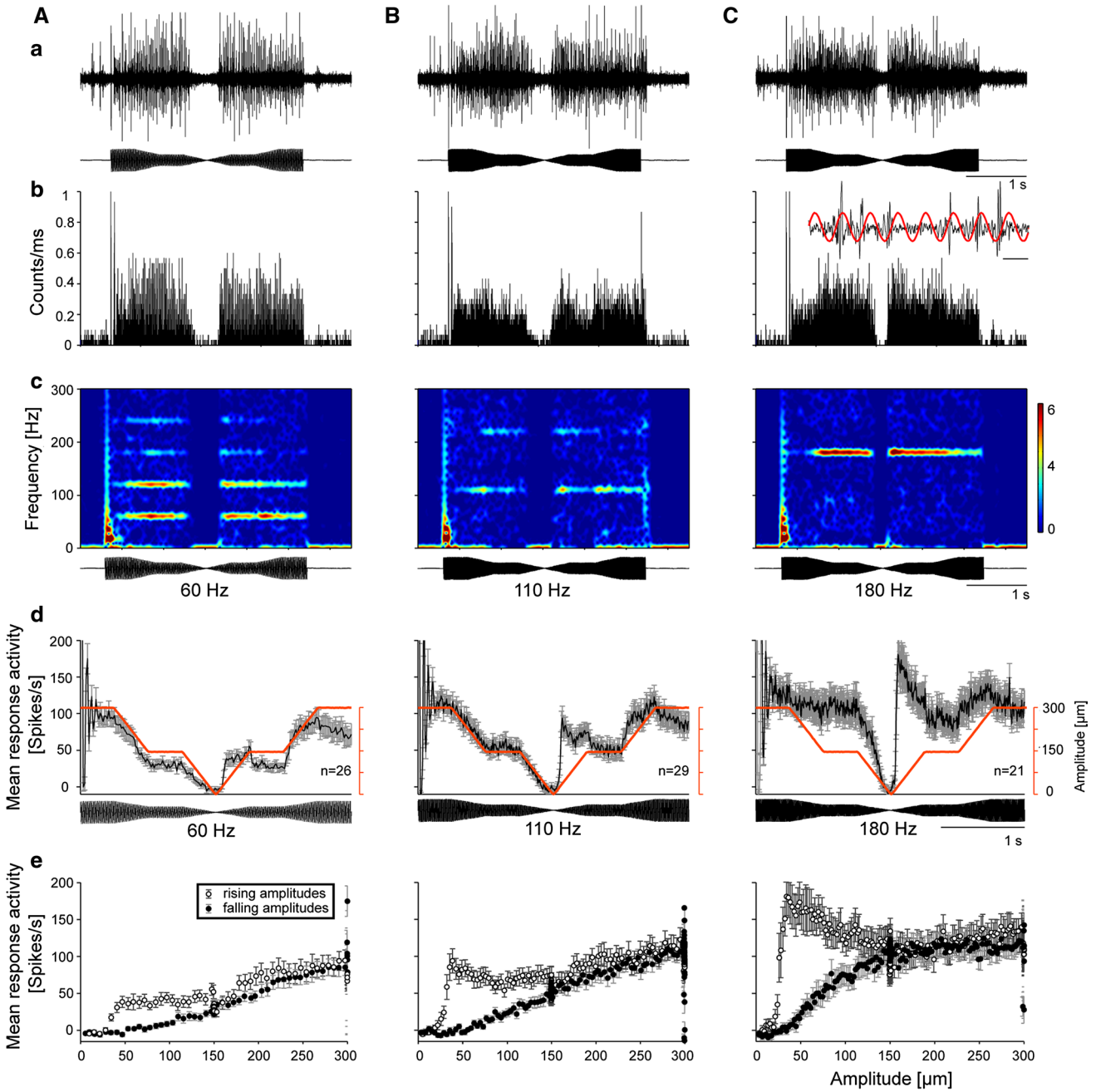

Fig. 2 Responses of cortical multi-units to amplitude-modulated whisker movements at vibratory frequencies of 60, 110 and 180 Hz, respectively (**A**–**C**). Analysis of a multi-unit (**a**–**c**), analysis of the population of multi-units showing responses with frequency coding by phase locking (**d**, **e**). *Row* **a**, raw spike and stimulus traces. *Row* **b**, PSTHs (bin width 1 ms) showing the mean of 50 consecutive responses. The *inset* shows a single trace of the phase-locked discharges of the multi-unit to 180 Hz vibration at high temporal resolution (*scale bar* 5 ms). *Row* **c**, time–frequency plots of the stimulus-locked activity showing the increase of evoked power (*colour scale* in arbitrary units) during stimulation (*bottom traces*). A band of increased power at the stimulation frequency is present in all cases. *Row* **d**, population mean discharge rates (spikes/s; ±SEM) during stimulation. *Red curves* show the profile of stimulus amplitude. *Row* **e**, population mean discharge rates (spikes/s; ±SEM) as a function of the movement amplitude for stimulation with falling amplitudes (*filled circles*) and rising amplitudes (*open circles*)

($p = 0.06$), indicating a long-lasting effect of stimulus onset and vibration frequency. These data demonstrate that movement amplitude cannot be the only factor determining the discharge rate (see Fig. 4a, b).

Frequency modulation

An example of a multi-unit with responses to FM stimulation is given in Fig. 3Aa–c, Ba–c. Following a marked

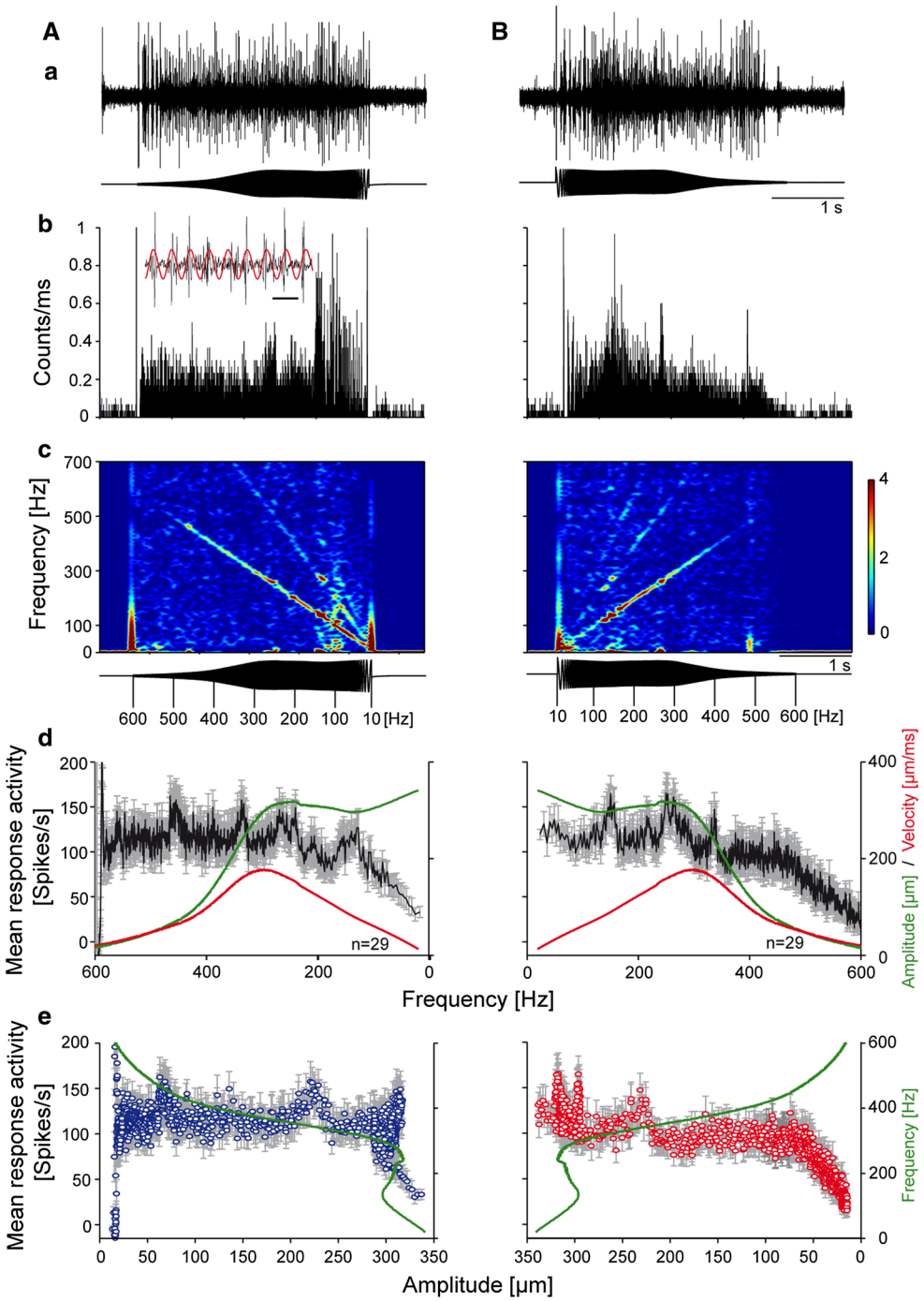

Fig. 3 Responses of cortical multi-units to 600–10 Hz descending (**A**) and 10–600 Hz ascending (**B**) frequency-modulated whisker movements. Analysis of a multi-unit (**a**–**c**) and analysis of the population of multi-units showing responses with frequency coding by phase locking (**d**, **e**). *Rows* **a**–**e**, raw spike and stimulus traces, PSTHs, time–frequency plots and stimulus traces, population mean discharge rates plotted as a function of stimulation frequency, and population mean discharge rates plotted as a function of movement amplitudes, respectively, are shown with the same conventions as in Fig. 2. *Row* **b** *inset*, single trace of the phase-locked discharges of the multi-unit to 134 Hz vibration at high temporal resolution (*scale bar* 10 ms). *Row* **c**, a band of increased power at the stimulation frequency is present for most of the frequency range. *Row* **d**, population mean response rates and overlays of the plots of amplitude (*green*) and velocity (*red*) as a function of vibration frequency. *Row* **e**, population mean discharge rates (spikes/s; ±SEM) and overlay of the plot of stimulation frequency as a function of movement amplitude for stimulation with descending frequencies (*left*) and ascending frequencies (*right*). Note that the mean velocity increases with frequency up to 302 Hz and then decreases for higher frequencies due to the decreasing amplitude of the stimulator movement (see stimulus traces in **a**, **c**, overlay in **d**, and Fig. 1). The duration of each stimulus was 3.2 s

ON-response, discharges entrained to the FM vibration occur throughout its duration (Fig. 3Aa, b, Ba, b). The phase-locked occurrence of the multi-unit discharges is shown for the stimulus part around 134 Hz in the inset of Fig. 3Ab. The time–frequency analysis revealed an increase of evoked power at the instantaneous stimulus frequency for a bandwidth covering a range of almost 600 Hz of vibration frequencies (during stimulation with descending frequencies, Fig. 3Ac). A detailed analysis of the encoded frequencies for all multi-units is presented further below (see Fig. 5d).

Since frequency and amplitude are changing concurrently during an FM stimulus, the discharge rates of all multi-units were plotted separately as a function of the frequency (Fig. 3Ad, Bd) and the amplitude (Fig. 3Ae, Be). There was a constant mean discharge rate of 120.0 ± 0.9 Hz for vibration frequencies between 580 and 240 Hz during descending FM stimulation and between 20 and 350 Hz during ascending FM stimulation, i.e., during the first 1.9 and 1.8 s of the stimulus, respectively. The response decrease in both cases towards stimulus end, therefore, could result from

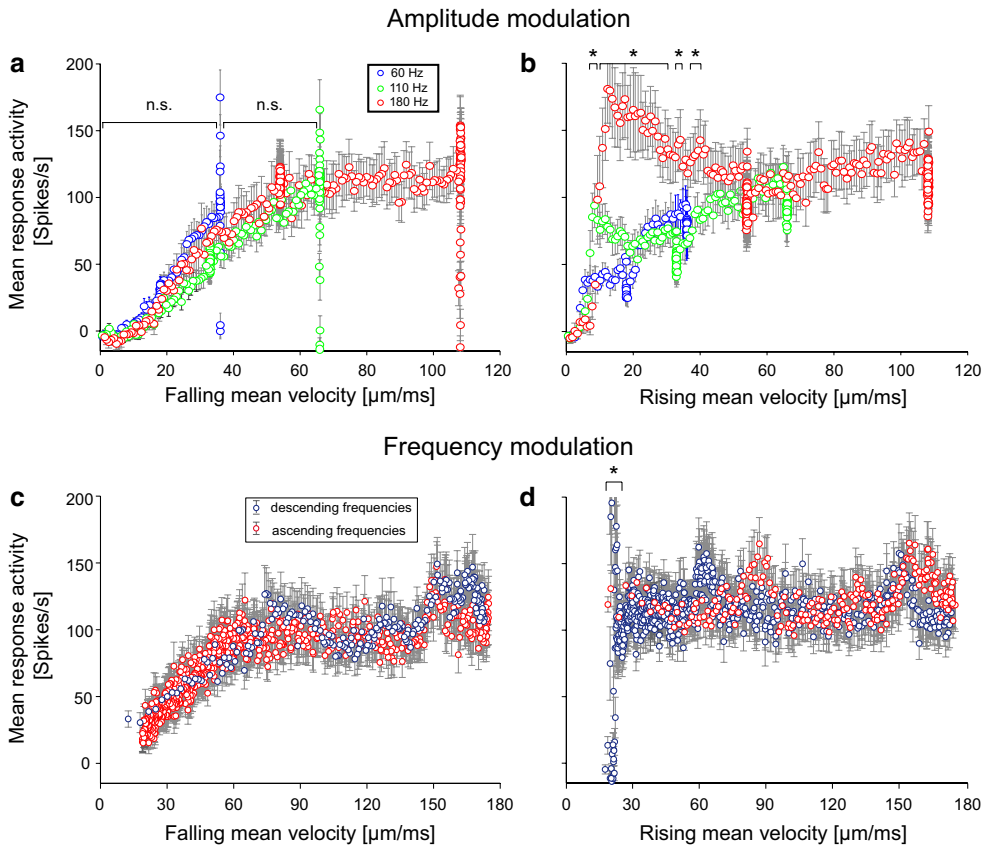

Fig. 4 Correlation of spike rate with stimulus velocity. The mean discharge rates (±SEM) from responses ($n = 76$) to the three AM stimuli are shown as a function of the mean falling (**a**) and rising (**b**) velocities. The mean discharge rates from responses ($n = 58$) to the two FM stimuli are shown as a function of the mean falling (**c**) and rising (**d**) velocities. An ANOVA was calculated for discharge rates elicited in response to stimuli with equal velocity, each pair of data tested had different p values, those below 0.01 are marked (*asterisk*)

adaptation during continuing stimulation. Alternatively, this could reflect a genuine decrease in the spike rate at vibration frequencies from 150 to 18 Hz in the first case and a decrease with the amplitude during ascending FM stimulation from 450 to 600 Hz in the second case, respectively. Comparison with the overlays of the plots of velocity and amplitude show, however, that in both cases the discharge decrease mirrors the decrease in velocity. Analysis of the correlation of the discharge rate with stimulus amplitude revealed relatively constant response rates over a wide range of amplitudes.

Taken together, the data indicate that in case of the descending FM stimulation, the spike rate indeed more faithfully codes for the frequency (and/or velocity) of vibration in the range of 150–18 Hz irrespective of the amplitude. In case of the ascending stimulation, the spike rate codes for the amplitude (and/or velocity) rather than the frequency of vibration in the high-frequency range (448–600 Hz). The distinct peaks of spike discharge during the first part of the stimuli (Fig. 3Ad, Bd) could reflect increased responses at resonance frequencies of different whiskers (Hartmann et al. 2003; Andermann et al. 2004; Neimark et al. 2003). However, separate analysis of the multi-units with primary whiskers B1, C1, C6 and E4, for example, revealed that these peaks occur at similar vibration frequencies for all neurons during descending and ascending FM stimulation and were elicited by slight changes in movement amplitude and hence velocity (see "Materials and methods" section; Fig. 1D, E).

Coding of movement velocity

As noted above, stimulus velocity may be a relevant factor represented by the spike rate. The mean discharge rate is positively correlated with the absolute mean velocity (mean velocity during a half cycle) during whisker movement with falling amplitudes (Fig. 4a). All discharge rates evoked by whisker movements with different frequencies but the same mean velocity were compared; these showed no significant differences except for periods during ON-responses (ANOVA, $p < 0.05$). Thus, the mean velocity of whisker vibration determines the cortical discharges at least

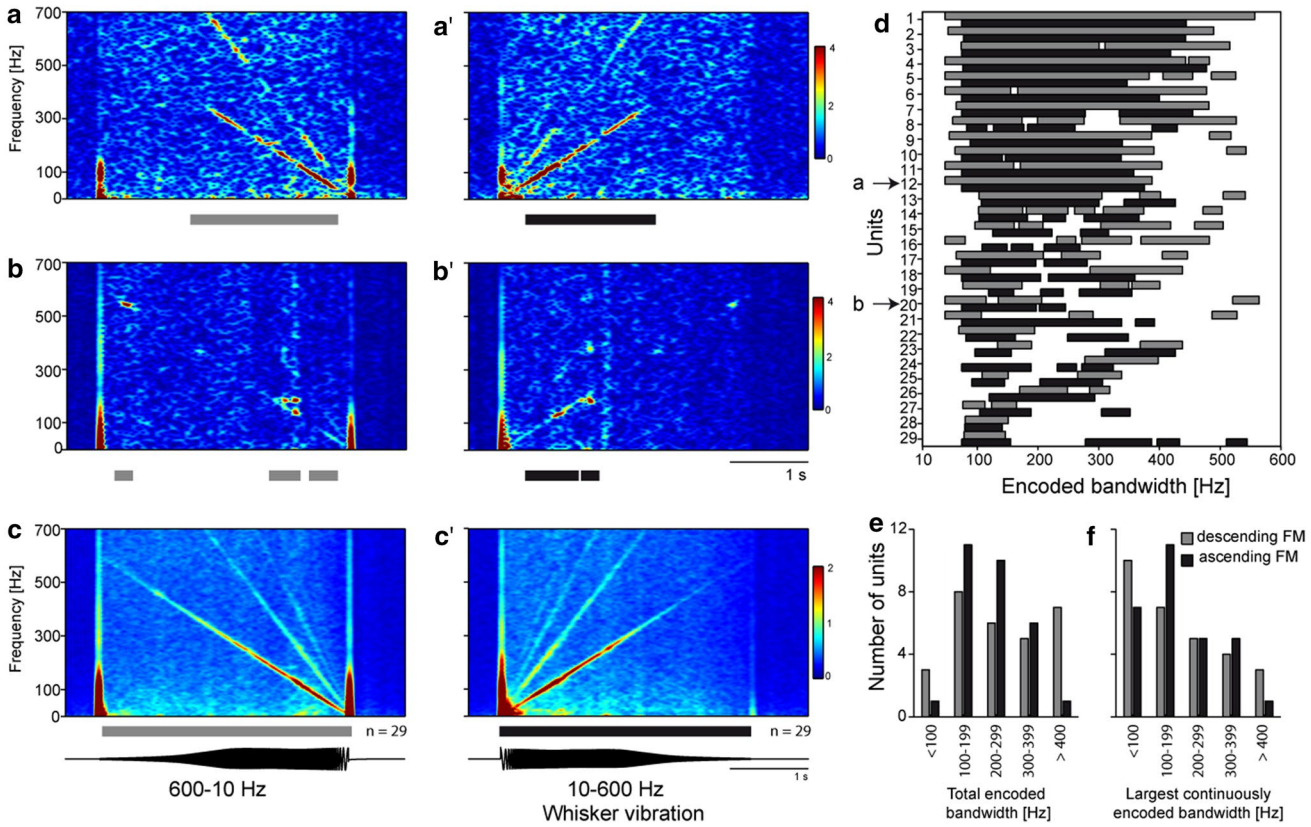

Fig. 5 Frequency coding by phase locking in responses to 10–600 Hz frequency-modulated whisker movements. Time frequency transformations of the evoked cortical activity to descending (**a**, **b**) and ascending (**a′**, **b′**) FM stimuli for two multi-units and for the population of 29 units (**c**, **c′**), respectively, are shown. The ranges of FM whisker movement where frequency coding occurred are labelled with *grey* (descending FM stimuli) and *black bars* (ascending FM stimuli). See "Materials and methods" section for assessment of frequency coding. The *colour scale* indicates power increase in arbitrary units. **d** The ranges where frequency coding occurred during descending (*grey bars*) and ascending (*black bars*) FM stimuli are marked for all 29 cortical units. The two units whose data are shown in **a**, **b** are marked with *arrows*. The units were assigned to five groups according to the total (**e**) and largest continuous (**f**) frequency range encoded in their responses

for movements with falling amplitudes and up to about 60 µm/ms, where saturation occurs at a discharge rate of 117.2 ± 1.9 spikes/s.

The results were the same when data from FM stimulation were analysed (Fig. 4c). Here, however, falling mean velocities occurred during stimulation with frequencies descending between 302 and 10 Hz and with frequencies ascending between 302 and 600 Hz (see "Materials and methods" section; Fig. 1Dc, Ec). Cortical responses to whisker vibrations with falling mean velocity were positively correlated with the mean velocity of movement, although again there is a ceiling effect towards high velocities above about 60 µm/ms. Comparisons of discharge rates evoked by the different stimuli showed additionally that they were independent of stimulation frequency (Fig. 4c; $p < 0.05$). However, for rising mean velocity of the whisker vibration during FM stimulation, this cannot be shown, rather discharge rates appear to be already at a maximum presumably because of the dominant ON-response (Fig. 4d). The dominance of the ON-response is visible during AM stimulation with rising velocity and here clearly dependent on stimulus frequency (Fig. 4b; $p < 0.05$).

These analyses show that the spike rate of a local population of cortical neurons for a wide range of movement frequencies, amplitudes and velocities is not the relevant stimulus code. Very subtle movements, however, with low amplitudes at high frequencies, and thus low velocities, as well as with high amplitudes at low frequencies, and thus also low velocities, are rate-coded.

Reflection of frequency bands in the population code

We thus asked whether a temporal code more reliably reflects whisker vibrations across a wider range and whether their frequency components are represented in a distributed pattern within the barrel cortex. The temporal precision of spike occurrence during FM whisker movements is revealed in time–frequency plots by an increase

of power at the instantaneous frequency (Figs. 3Ac, Bc, 5). Such periods of increases were tested for significance (see "Materials and methods" section; $p < 0.05$) and the bandwidths of significant frequencies were marked in responses of 29 multi-units with grey and black bars for descending and ascending FM stimuli, respectively (Fig. 5d). Examples for coding of a wide band of frequencies (18–400 Hz) and of a rather small bandwidth (18–200 Hz) are shown in Fig. 5a,a′, b,b′, respectively. The entire range of instantaneous frequencies was found to be covered during descending (Fig. 5c) and ascending FM stimulation (Fig. 5c′) when the population activity of all 29 multi-units was analysed. Most of the multi-units coded for frequencies with more than 100 Hz bandwidth (Fig. 5e). In some cases, a few frequencies were encoded intermittently, however, two-thirds of the multi-units covered a continuous bandwidth of over 100 Hz and some of up to 550 Hz (Fig. 5f). Although the frequencies encoded during descending and ascending FM whisker movements were not always identical, the mean bandwidth of encoded frequencies did not differ between these stimuli.

Taken together, the data indicate that complex textures comprising a variety of frequency components can be encoded by a local small group of cortical neurons. Furthermore, there was no association of the width of encoded frequencies with the neurons' receptive field of large or small whiskers and of upper or lower rows. Large bandwidths were found, for example, for receptive fields composed of the principle whiskers Gamma, A2, C4, D4 and E3.

Reflection of frequency bands in single-unit activity

The representation of wide bands of vibration frequencies still could be generated by an assembly of single-unit activity each covering relatively small bands of differing frequencies, i.e., with narrow tuning curves. This hypothesis could be tested by analysing single-units. Sorting single-units from the multi-units of our data, however, was flawed because of the highly phase-locked occurrence of the spikes. This resulted in superposition of spikes from different units, which did not allow to unambiguously identify individual waveforms and amplitudes in most cases. One of the 19 clean examples is shown in Fig. 6. Original traces of the multi-unit recording to descending (Fig. 6a, left) and ascending (Fig. 6a, right) FM whisker vibration are shown, and analyses were obtained for time stamps of the single-unit whose waveform is displayed in Fig. 6b, right (overlay of fifty consecutive spikes). The phase-locked occurrence of the spikes is shown for the stimulus parts around 539 and 485 Hz (Fig. 6b). The spike occurrence, however, shifted gradually along the phase with descending or ascending frequency (Fig. 6c), due to changing stimulus velocity and/or latency of spike elicitation. For a corresponding range of frequencies, the time–frequency analyses (Fig. 6d) demonstrate significant temporal coding for descending (grey bar, 18–450 Hz; $p < 0.05$) and ascending frequencies (black bar, 100–400 Hz; $p < 0.05$) of whisker movements. In 10 of the 19 single-units coding of stimulus frequency by phase locking was detected by these analyses and eight coded for more than 100 Hz bandwidth up to 470 Hz. This demonstrates that wide continuous bands of frequencies can indeed be encoded by single-units of the barrel cortex.

Frequency coding by phase locking and gamma band activity

In addition to the activity evoked at the stimulation frequency, activity was induced with a significant peak in the low gamma band range (~40 Hz), as shown by the two examples of multi-units in Fig. 7a, b. Gamma band activity did not occur during low-frequency stimulation (below 100 Hz), but was most prominent during high-frequency stimulation (300–500 Hz; Fig. 7a′). The ranges of stimulus frequencies inducing gamma band activity appeared to only partially overlap with those where frequency coding by phase locking predominated (red and blue bars below the graphs ($p < 0.05$), respectively). This was analysed further for 13 multi-units (Fig. 7c, d). Clearly, frequency coding by phase locking is dominant in the range of vibration from 10 to about 400 Hz, although present up to 550 Hz. In contrast, the probability of the occurrence of gamma band oscillations increases towards higher-frequency stimulation. This applies to both the descending and ascending stimulation frequencies.

Discussion

Vibrating single whiskers for 3.2 s with frequencies modulated between 10 and 600 Hz elicited responses in S1 neurons closely following these stimuli by the phase-locked occurrence of spike discharges. This suggests that vibratory movements of whiskers can be represented by a temporal code. Small groups of neurons therefore may encode more than 500 Hz vibratory bandwidth, and, in turn, single whiskers may transmit information about a wide range of frequencies. The analysis of amplitude- and frequency-modulated stimuli showed that a rate code may serve to represent the velocity of whisker movement, however, only up to about 60 µm/ms, corresponding to vibration in ranges of about 180–10 Hz at 336 µm amplitude or 400–600 Hz at 200–16 µm. Frequency and velocity of high-amplitude movements (up to 330 µm) were reflected by the discharge rate, but only in the low-frequency range (up to 180 Hz). In the high-frequency range (400–600 Hz), the movement velocity was correlated with the discharge

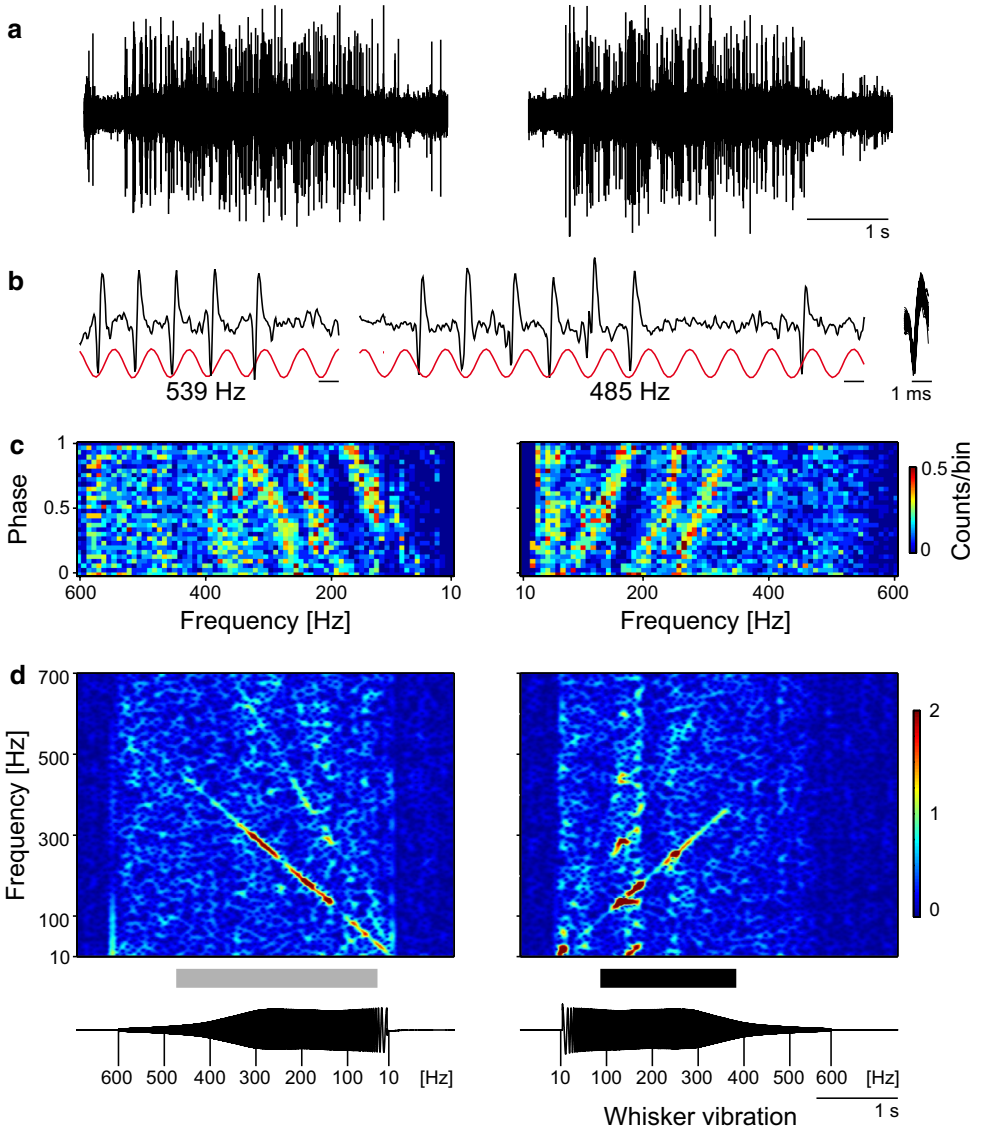

Fig. 6 Responses of a single-unit to 10–600 Hz FM vibration. **a** Spike record of the responses of a multi-unit to descending (*left*) and ascending (*right*) stimulus frequencies (stimulus traces at *bottom*) from which a single-unit was sorted (see **b** *right*, overlay of 50 consecutive spike waveforms). **b** Single traces of the phase-locked occurrence of spikes at high temporal resolution for the stimulus part around 539 and 485 Hz. **c** Raster plots of the spike counts (*colour scale*) of the single-unit occurring at a certain phase of the vibratory cycle (12°/bin) versus vibration frequency (8 Hz/bin). Note the gradual shift along the vibratory cycle as the frequency descends or ascends. **d** Time–frequency plots of the responses of the single-unit, the *colour scale* indicates power increase in arbitrary units. The *grey* (descending FM stimulus) and the *black* (ascending FM stimulus) *bars* indicate the ranges of frequency coding (see "Materials and methods" section for assessment of frequency coding by phase locking) and the *bottom traces* show the stimulus profiles

rate for low-amplitude movements (<200 μm); movement frequency, however, was not rate-coded, but reflected by the phase locking of spikes. In addition, oscillatory activity in the gamma band range increased with higher stimulus frequencies.

These results support the notion that different aspects of cortical activity may encode surface roughness and mediate texture perception (Salinas et al. 2000; Melzer et al. 2006; Hollins and Bensmaia 2007; Lottem and Azouz 2008; Boloori et al. 2010; Jadhav and Feldman 2010; Lundstrom et al. 2010; Panzeri et al. 2010). A rate code alone, as suggested in many studies (Hernandez et al. 2000; Arabzadeh et al. 2003, 2006; Luna et al. 2005), may not suffice to allow discrimination among fine-grained textures. Roughness, here defined as the size and spacing of texture elements, varies over wide ranges. It is conceivable that separate encoding mechanisms operate in different ranges along a feature dimension. In analogy to the mechanisms suggested for roughness perception in humans (Hollins and Bensmaia 2007), a spatial code, i.e., integration of information from several neighbouring whiskers, may be used for processing of coarse surfaces and a vibrotactile code may represent very fine surfaces. A major role for spike timing in coding of whisker information in fact has been proposed from application of information-theoretic methods (Petersen et al. 2009).

The high precision of spike timing during prolonged stimulation found here and in our previous study for barrel cortex neurons (Ewert et al. 2008) was surprising in light of other reports. The exquisite precision present in discharges from primary afferent fibres in the range of <1 ms (Gibson and Welker 1983; Jones et al. 2004a, b, 2006; Lottem and Azouz 2008, 2009; Bale et al. 2013)

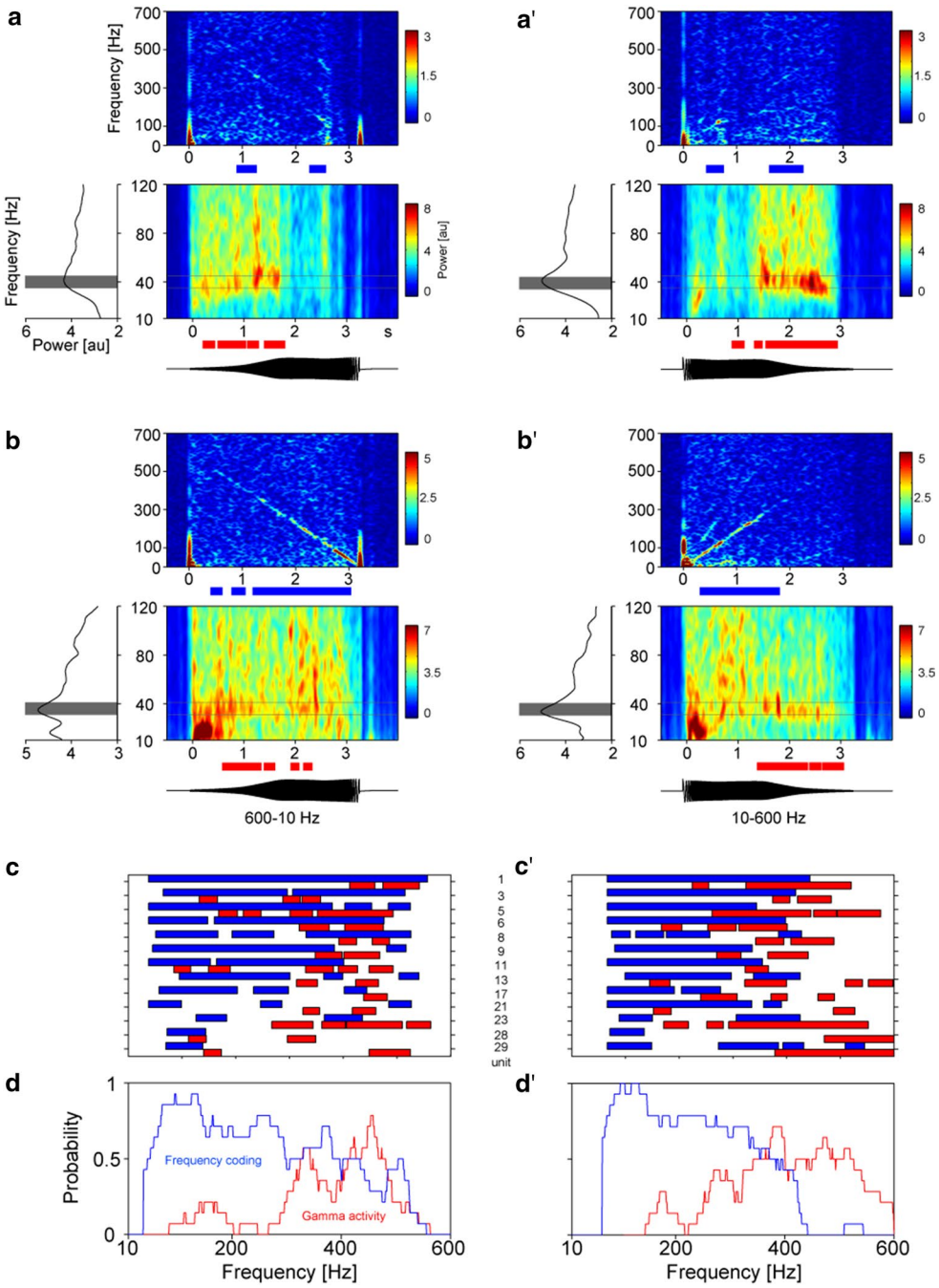

Fig. 7 Time–frequency analysis of evoked and induced power of cortical responses to FM whisker vibration. Two examples are given for descending (**a**, **b**) and ascending (**a′**, **b′**) FM stimuli, with *blue bars below the graphs* of the evoked activity (*upper*) indicating periods of frequency coding by phase locking ($p < 0.05$). The induced activity (*lower*) is shown in time–frequency plots and as the mean power across all frequencies. Here, the peak value ±5 Hz (*shaded* in *gray*) was tested at each point in time for significantly higher values ($p < 0.05$, *red bars*) in relation to ±30 Hz outside this range. The *colour scale* indicates power increase in arbitrary units. The occurrence of frequency coding (*blue bars*) and increase in gamma band activity (*red bars*) is shown for 13 multi-units during descending and ascending FM stimulation (**c**, **c′**) as well as the probability of frequency coding (*blue*) and increased gamma band activity (*red*) in this neuronal group (**d**, **d′**)

or even <10 µs (Gottschaldt and Vahle-Hinz 1981) was shown to be preserved in the ascending pathway through the principal trigeminal nucleus (Deschênes et al. 2003) and the thalamic VPM (Vahle-Hinz and Gottschaldt 1983; Castro-Alamancos 2002; Deschênes et al. 2003; Montemurro et al. 2007; Vahle-Hinz et al. 2007), but not in S1 cortex. Here, studies on anesthetized animals reported spiking precision of at the most a few or tens of milliseconds and phase locking if at all only up to about 40 Hz whisker vibration (Garabedian et al. 2003; Khatri et al. 2004; Kleinfeld et al. 2006). Moreover, sensory adaptation to continuing stimulation or to increased input frequency was described as a prominent characteristic of S1 neurons in anesthetized animals (Andermann et al. 2004; Khatri et al. 2004; Kleinfeld et al. 2006; Maravall et al. 2007). However, this was shown to be dependent on global cortical activity and behaviour (Castro-Alamancos 2002, 2004; Petersen et al. 2009). In particular, the results of many of the studies cited above may have been biased by the largely depressive effect of the anaesthesia, the consequences of which have been discussed in detail by Ewert et al. (2008).

Given the high precision in spike timing of primary afferents, it is astounding that this could be passed on via three synapses to cortical neurons. Petersen et al. (2009) suggest that high-velocity components of stimuli such as step deflections at stimulus onset or high-frequency vibrations induce large, transient membrane currents which in turn rapidly increase membrane potential above spike threshold. Therefore, variation in spike generation is minimal in mechanoreceptors. This signal is passed on to VPM cells because the lemniscal synapses form multiple contacts along the primary dendrites and thus are very potent (Brecht and Sakmann 2002; Castro-Alamancos 2002; Deschênes et al. 2003). Although thalamocortical synapses are much weaker (Gil et al. 1999; Bruno and Sakmann 2006), thalamocortical synaptic transmission has been shown to be highly conserved across different brain states (Stoelzel et al. 2009). The robust, synchronous firing of VPM neurons to high-velocity events again induces high-amplitude EPSPs which fire precisely timed cortical spikes, which is not the case for low-velocity stimuli. Such low-velocity stimuli occurred in our study during movements with low amplitudes at high frequencies, as well as with high amplitudes at low frequencies resulting in a linear representation of velocity in the discharge rate of S1 neurons. A rate code for stimulus velocity was also suggested by Arabzadeh et al. (2003, 2006). SA1 mechanoreceptors are activated by such subtle movements (Gottschaldt and Vahle-Hinz 1981; Gibson and Welker 1983; Jones et al. 2004b; Stüttgen et al. 2006); an indication of their involvement is present in the ON-responses to rising AM stimuli (see Figs. 2, 4b) where low velocities elicited the largest responses. On the other hand, the higher harmonics to the stimulation frequencies present in the time–frequency plots (Figs. 2Ac, 3Ac, Bc) indicate that phase-locked responses occurred at both half cycles of the sine waves, which may have resulted from activation of non-directionally sensitive SA- and RA mechanoreceptors (Lichtenstein et al. 1990; Gottschaldt and Vahle-Hinz 1981).

Apart from the robust and intensified transmission of the immediate responses to the onset of stimuli along the ascending pathway, as discussed above, long-lasting (~0.5 s) response increases followed those ON-responses both to high frequencies in the falling frequency case and to low frequencies in the rising frequency case (FM stimuli, Fig. 3). When compared with the velocity profile, it is evident that these long-lasting increases occur in response to rising mean velocities in all cases (also to AM stimuli, Fig. 2). In addition to response properties of the peripheral mechanoreceptors as discussed above, thalamic and/or cortical dynamical processes may further serve to enhance movement responses over a longer time period. This may reflect mechanisms of adaptation over 100s of milliseconds as demonstrated by Maravall et al. (2007). This type of adaptation on a slow time scale was shown to adjust the gain of neuronal coding with changes in stimulus distribution. Maravall et al. (2007) suggested that in cases where stimulus magnitude was the same, and thus rate coding would fail to detect finer details of textures, these may be represented by the temporal discharge pattern. Whether oscillatory activity may play a role in these mechanisms of adaptive gain rescaling remains to be determined.

An important question is whether high-frequency vibrations in the range studied here do occur during active probing of textures and play a role at all for perception. Indeed, when whiskers sweep across a surface, its roughness is translated into high-frequency micro motions or stick–slip events which occur superimposed upon the macro motions during active whisking (Arabzadeh et al. 2003; Hipp et al. 2006; Lottem and Azouz 2008, 2009; Ritt et al. 2008; Wolfe et al. 2008; Jadhav et al. 2009). The slips have been shown to correlate in rate and magnitude with the surface roughness (Lottem and Azouz 2009) and to drive spikes in S1 cortex with high temporal precision (15–20 ms jitter; Jadhav et al. 2009). For a phase-locked response to 550 Hz vibration as found in the present study, an even higher temporal precision of <1 ms is required. Such submillisecond precision of spike timing has been demonstrated for neurons of the thalamic VPM (Montemurro et al. 2007). When the suppressive effects of the anaesthesia are considered, it is likely that the tactile system may be capable of coding even higher frequencies than reported here.

Although the situation with passive stimulation of whiskers in anaesthetized or awake preparations is far from the actively exploring animal, studies using these preparations may still be of relevance because stimulus parameters are highly controlled, and translation of high-frequency components of surfaces have been shown to be similar during active and passive whisker motions (Lottem and Azouz 2009), and at least in some instances, rats maintain contact with a texture and use passive movement by the texture without whisking during exploration (Ritt et al. 2008).

The correlated firing of neuronal populations in the gamma band range has been suggested to underlie assembly formation by neural coherence in sensory systems (Engel et al. 1992, 2001; Singer and Gray 1995; Herrmann et al. 2004). Also in the somatosensory system of rats, gamma band oscillations have been reported to occur during passive whisker stimulation or tactile exploration (Nicolelis et al. 1995; Miyashita and Hamada 1996; Jones and Barth 1997; Hamada et al. 1999). Its functional relevance, however, is still a matter of debate. Our data may suggest that the detection of very fast signals may rely on the coordinated oscillatory activity within the neuronal population. For very fast stimulus frequencies, phase locking of barrel cortex neurons to stimulus transients may become less reliable, and thus, intrinsically coordinated

rhythms may become more prominent in the population activity.

In conclusion, we present data that neurons in the barrel cortex encode rapidly changing vibratory movements of whiskers by precisely phase-locked spiking activity up to 550 Hz vibratory frequency. Given the capability of the peripheral mechanoreceptors to cover frequencies into the thousands of hertz, it is likely that cortical neurons in the awake animal also encode a much wider range of vibratory movements. Whether non-phase-locked oscillatory population activity has relevance for encoding of textures remains to be determined. In addition to this temporal code representing whisker vibration, movement velocity may be encoded by the rate of spike discharges, particularly for low velocities. Thus, both a temporal code and a rate code may operate in a complementary fashion to encode complex signals induced by whisker movements during exploration of surface textures.

Acknowledgments This work was supported by the European Union (IST-2000-28127) and the German Research Foundation (SFB 936/Z1).

Conflict of interest The authors declare that they have no conflict of interest.

References

Andermann ML, Ritt J, Neimark MA, Moore CI (2004) Neural correlates of vibrissa resonance: band-pass and somatotopic representation of high-frequency stimuli. Neuron 42:451–463

Andres KH (1966) Über die Feinstruktur der Rezeptoren in Sinushaaren. Z Zellforsch 75:339–365

Arabzadeh E, Petersen RS, Diamond ME (2003) Encoding of whisker vibration by rat barrel cortex neurons: implications for texture discrimination. J Neurosci 23:9146–9154

Arabzadeh E, Panzeri S, Diamond ME (2006) Deciphering the spike train of a sensory neuron: counts and temporal patterns in the rat whisker pathway. J Neurosci 26:9216–9226

Bale MR, Davies K, Freeman OJ, Ince RAA, Petersen RS (2013) Low-dimensional sensory feature representation by trigeminal primary afferents. J Neurosci 33:12003–12012

Boloori A-R, Jenks RA, Desbordes G, Stanley GB (2010) Encoding and decoding cortical representations of tactile features in the vibrissa system. J Neurosci 30:9990–10005

Brecht M, Sakmann B (2002) Whisker maps of neuronal subclasses of the rat ventral posterior medial thalamus, identified by whole-cell voltage recording and morphological reconstruction. J Physiol 538:495–515

Bruno RM, Sakmann B (2006) Cortex is driven by weak but synchronously active thalamocortical synapses. Science 312:1622–1627

Carvell GE, Simons DJ (1990) Biometric analyses of vibrissal tactile discrimination in the rat. J Neurosci 10:2638–2648

Castro-Alamancos MA (2002) Different temporal processing of sensory inputs in the rat thalamus during quiescent and information processing states in vivo. J Physiol 539:567–578

Castro-Alamancos MA (2004) Absence of rapid sensory adaptation in neocortex during information processing states. Neuron 41:455–464

Deschênes M, Timofeeva E, Lavallee P (2003) The relay of high-frequency sensory signals in the whisker-to-barreloid pathway. J Neurosci 23:6778–6787

Engel AK, König P, Kreiter AK, Schillen TB, Singer W (1992) Temporal coding in the visual cortex: new vistas on integration in the nervous system. Trends Neurosci 15:218–226

Engel AK, Fries P, Singer W (2001) Dynamic predictions: oscillations and synchrony in top-down processing. Nat Rev Neurosci 2:704–716

Ewert TAS, Vahle-Hinc C, Engel AK (2008) High-frequency whisker vibration is encoded by phase-locked responses of neurons in the rat's barrel cortex. J Neurosci 28:5359–5368

Garabedian CE, Jones SR, Merzenich MM, Dale A, Moore CI (2003) Band-pass response properties of rat SI neurons. J Neurophysiol 90:1379–1391

Gibson JM, Welker WI (1983) Quantitative studies of stimulus coding in first-order vibrissa afferents of rats. 2. Adaptation and coding of stimulus parameters. Somatosens Res 1:95–117

Gil Z, Connors BW, Amitai Y (1999) Efficacy of thalamocortical and intracortical synaptic connections: quanta, innervation, and reliability. Neuron 23:385–397

Gottschaldt KM, Vahle-Hinz C (1981) Merkel cell receptors: structure and transducer function. Science 214:183–186

Guic-Robles E, Valdivieso C, Guajardo G (1989) Rats can learn a roughness discrimination using only their vibrissal system. Behav Brain Res 31:285–289

Hamada Y, Miyashita E, Tanaka H (1999) Gamma-band oscillations in the "barrel cortex" precede rat's exploratory whisking. Neuroscience 88:667–671

Hartmann MJ, Johnson NJ, Towal RB, Assad C (2003) Mechanical characteristics of rat vibrissae: resonant frequencies and damping in isolated whiskers and in the awake behaving animal. J Neurosci 23:6510–6519

Hernandez A, Zainos A, Romo R (2000) Neural correlates of sensory discrimination in the somatosensory cortex. Proc Natl Acad Sci 97:6191–6196

Herrmann CS, Munk MHJ, Engel AK (2004) Cognitive functions of gamma-band activity: memory match and utilization. Trends Cogn Sci 8:347–355

Hipp J, Arabzadeh E, Zorkin E, Conradt J, Kayser C, Diamond ME (2006) Texture signals in whisker vibrations. J Neurophysiol 95:1792–1799

Hollins M, Bensmaia SJ (2007) The coding of roughness. Can J Exp Psychol 61:184–195

Jadhav SP, Feldman DE (2010) Texture coding in the whisker system. Curr Opin Neurobiol 20:313–318

Jadhav SP, Wolfe J, Feldman DE (2009) Sparse temporal coding of elementary tactile features during active whisker sensation. Nat Neurosci 12:792–800

Jones MS, Barth DS (1997) Sensory-evoked high-frequency (γ-band) oscillating potentials in somatosensory cortex of the unanesthetized rat. Brain Res 768:167–176

Jones LM, Depireux DA, Simons DJ, Keller A (2004a) Robust temporal coding in the trigeminal system. Science 304:1986–1989

Jones LM, Lee S, Trageser JC, Simons DJ, Keller A (2004b) Precise temporal responses in whisker trigeminal neurons. J Neurophysiol 92:665–668

Jones LM, Kwegyir-Afful EE, Keller A (2006) Whisker primary afferents encode temporal frequency of moving gratings. Somatosens Mot Res 23:45–54

Khatri V, Hartings JA, Simons DJ (2004) Adaptation in thalamic barreloid and cortical barrel neurons to periodic whisker deflections varying in frequency and velocity. J Neurophysiol 92:3244–3254

Kleinfeld D, Ahissar E, Diamond ME (2006) Active sensation: insights from the rodent vibrissa sensorimotor system. Curr Opin Neurobiol 16:435–444

Krupa DJ, Matell MS, Brisben AJ, Oliveira LM, Nicolelis MAL (2001) Behavioral properties of the trigeminal somatosensory system in rats performing whisker-dependent tactile discriminations. J Neurosci 21:5752–5763

Lichtenstein SH, Carvell GE, Simons DJ (1990) Responses of rat trigemnal ganglion neurons to movements of vibrissae in different directions. Somatosens Motor Res 7:47–65

Lottem E, Azouz R (2008) Dynamic translation of surface coarseness into whisker vibrations. J Neurophysiol 100:2852–2865

Lottem E, Azouz R (2009) Mechanisms of tactile information transmission through whisker vibrations. J Neurosci 29:11686–11697

Luna R, Hernandez A, Brody CD, Romo R (2005) Neural codes for perceptual discrimination in primary somatosensory cortex. Nat Neurosci 8:1210–1219

Lundstrom BN, Fairhall AL, Maravall M (2010) Multiple timescale encoding of slowly varying whisker stimulus envelope in cortical and thalamic neurons in vivo. J Neurosci 30:5071–5077

Maravall M, Petersen RS, Fairhall AL, Arabzadeh E, Diamond ME (2007) Shifts in coding properties and maintenance of information transmission during adaptation in barrel cortex. PLoS Biol 5:0323–0334

Melzer P, Champney GC, Maguire MJ, Ebner FF (2006) Rate code and temporal code for frequency of whisker stimulation in rat primary and secondary somatic sensory cortex. Exp Brain Res 172:370–386

Metha SB, Kleinfeld D (2004) Frisking the whiskers: patterned sensory input in the rat vibrissa system. Neuron 41:181–184

Miyashita E, Hamada Y (1996) The 'functional connection' of neurones in relation to behavioural states in rats. NeuroReport 7:2407–2411

Montemurro MA, Panzeri S, Maravall M, Alenda A, Bale MR, Brambilla M, Petersen RS (2007) Role of precise spike timing in coding of dynamic vibrissa stimuli in somatosensory thalamus. J Neurophys 98:1871–1882

Moore CI (2004) Frequency-dependent processing in the vibrissa sensory system. J Neurophysiol 91:2390–2399

Neimark MA, Andermann ML, Hopfield JJ, Moore CI (2003) Vibrissa resonance as a transduction mechanism for tactile encoding. J Neurosci 23:6499–6509

Nicolelis MAL, Baccala LA, Lin RCS, Chapin JK (1995) Sensorimotor encoding by synchronous neural ensemble activity at multiple levels of the somatosensory system. Science 268:1353–1358

Panzeri S, Brunel N, Logothetis NK, Kayser C (2010) Sensory neural codes using multiplexed temporal scales. Trends Neurosci 33:111–120

Petersen RS, Panzeri S, Maravall M (2009) Neural coding and contextual influences in the whisker system. Biol Cybern 100:427–446

Rice FL, Fundin BT, Arvidsson J, Aldskogius H, Johansson O (1997) Comprehensive immunofluorescence and lectin binding analysis of vibrissal follicle sinus complex innervation in the mystacial pad of the rat. J Comp Neurol 385:149–184

Ritt JT, Andermann ML, Moore CI (2008) Embodied information processing: vibrissa mechanics and texture features shape micromotions in actively sensing rats. Neuron 57:599–613

Salinas E, Hernandez A, Zainos A, Romo R (2000) Periodicity and firing rate as candidate neural codes for the frequency of vibrotactile stimuli. J Neurosci 20:5503–5515

Singer W, Gray CM (1995) Visual feature integration and the temporal correlation hypothesis. Annu Rev Neurosci 18:555–586

Stoelzel CR, Bereshpolova Y, Swadlow HA (2009) Stability of thalamocortical synaptic transmission across awake brain states. J Neurosci 29:6851–6859

Stüttgen MC, Rüter J, Schwarz C (2006) Two psychophysical channels of whisker deflection in rats align with two neuronal classes of primary afferents. J Neurosci 26:7933–7941

Tallon-Baudry C, Bertrand O (1999) Oscillatory gamma activity in humans and its role in object representation. Trends Cogn Sci 3:151–162

Vahle-Hinz C, Gottschaldt KM (1983) Principal differences in the organization of the thalamic face representation in rodents and felids. In: Macchi G, Rustioni A, Spreafico R (eds) Somatosensory integration in the thalamus. Elsevier, Amsterdam, pp 125–145

Vahle-Hinz C, Detsch O, Siemers M, Kochs E (2007) Contributions of GABAergic and glutamatergic mechanisms to isoflurane-induced suppression of thalamic somatosensory information transfer. Exp Brain Res 176:159–172

Wolfe J, Hill DN, Pahlavan S, Drew PJ, Kleinfeld D, Feldman DE (2008) Texture coding in the rat whisker system: slip-stick versus differential resonance. PLoS Biol 6:1661–1677